Friction forces arising from fluctuating thermal fields

Jorge R. Zurita-Sánchez
The Institute of Optics, University of Rochester, Rochester, New York 14627, USA

Jean-Jacques Greffet
Laboratoire Énergétique Moléculaire et Macroscopique, Combustion, École Centrale Paris, 92295 Châtenay-Malabry Cedex, France

Lukas Novotny
The Institute of Optics, University of Rochester, Rochester, New York 14627, USA
(Received 16 August 2003; published 24 February 2004)

We calculate the damping of a classical oscillator induced by the electromagnetic field generated by thermally fluctuating currents in the environment. The fluctuation-dissipation theorem is applied to derive the linear-velocity damping coefficient γ. It turns out that γ is the result of fourth-order correlation functions. The theory is applied to a particle oscillating parallel to a flat substrate and numerical values for γ are evaluated for particle and substrate materials made of silver and glass. We find that losses are much higher for dielectric materials than for metals because of the higher resistivity. We predict that measurements performed on metal films are strongly affected by the underlying dielectric substrate and we show that our theory reproduces existing theoretical results in the nonretarded limit. The theory provides an explanation for the observed distance-dependent damping in shear-force microscopy and it gives guidance for future experiments. Also, the theory should be of importance for the design of nanoscale mechanical systems and for understanding the trade-offs of miniaturization.

DOI: 10.1103/PhysRevA.69.022902 PACS number(s): 79.20.Rf, 34.50.Bw

I. INTRODUCTION

The dynamics of an arbitrary system is affected by the system's interaction with the environment. The strength of the interaction limits the time window in which the system can be fully controlled. The interaction with the environment cannot be avoided since even in vacuum a system interacts with zero-point fluctuations. In order to understand the consequences of miniaturization it is important to understand how these external fluctuations affect a nanoscale system. For example, it has been explored to what extent Casimir forces influence the performance of micrometer-sized mechanical devices [1,2] and how external noise affects decoherence in ion traps [3]. Furthermore, various scanning probe techniques such as atomic force or near-field optical microscopies rely on the sensitivity of a local probe to pico-Newton forces. A theoretical understanding of underlying probe-sample interactions is necessary to assess the ultimate achievable sensitivity.

Fluctuating electromagnetic fields are not only generated by the vacuum but also by thermally activated currents in matter. These thermally excited fields interact with a dynamical system, such as a moving object, and give rise to a frictional force (Brownian motion). Therefore, any system comes necessarily to a statistical rest at finite temperatures. In this study, we theoretically investigate this dissipative force. We consider a small particle moving in a potential and interacting with the electromagnetic field produced by thermally excited currents in the environment. The friction experienced by the object is not produced by mechanical contact, but *only* by the fluctuating field.

Electromagnetically induced friction forces have been the subject of several theoretical studies. For example, Einstein *et al.* calculated the damping coefficient acting on an atom in free space in order to find a situation for which the Planck's energy spectrum arises naturally [4,5] (a detailed review of these papers is found in Refs. [6,7]). Some recent studies were aimed at deriving the friction force arising from the relative motion of two half-spaces separated by a small distance [8–12], and the damping of the motion of an atom or molecule close to a planar interface is derived in Refs. [13–17] (for a review see Ref. [18]). In the nonretarded limit where interactions occur instantaneously, the theory of Volokitin and Persson [16] reproduces the results obtained by Tomassone and Widom [14]. Our theory shows the same correspondence but we find an additional term which can be predominant for certain probe-sample material combinations. We derive numerical results for particles and substrates made of combinations of silver and glass and we show that friction forces are much stronger for dielectric materials.

Our theoretical study closely relates to recent experiments which deal with nanoscale probes in ultrahigh-vacuum conditions. These probes experience a friction force which depends strongly on the probe's proximity to the surface of a substrate as well as on the temperature of the environment [19–22]. The linear-velocity damping constant γ of a tip in the proximity of a planar surface has been measured by using different experimental configurations. Karrai and Tiemann used a tuning fork in which the attached tip was moving parallel to the surface [19]. Similar experiments with increased sensitivity have been performed by Stipe *et al.* using a vertical cantilever oscillating parallel to the surface [20]. On the other hand, Dorofeyev *et al.* [21] and Gotsmann and Fuchs [22] considered a tip moving in the normal direction to the surface. In all these experiments, the damping coefficient was measured in a range of $\approx 5-100$ nm. Other inter-

action mechanisms prevail at much shorter distances (e.g., see Ref. [23]). In many experimental situations measurements were *not* performed on bulk metal substrates but on metal films deposited on a dielectric substrate [20–22]. These experiments render damping coefficients that are many orders of magnitude larger than calculated values for bulk metal substrates [12,16,24]. Because of this large discrepancy, it is still unclear whether thermal fields are responsible for the observed friction forces at large distances.

In this article, we calculate the linear-velocity damping coefficient γ experienced by a polarizable particle trapped in a potential. The damping is generated through the interaction with electromagnetic fields caused by fluctuating thermal currents in the environment. The motion of the particle is modeled *classically* while the properties of the electromagnetic field are consistent with *quantum* theory. The formalism is valid for systems in *thermal equilibrium* and in the limit of weak coupling between particle and electromagnetic field. Furthermore, it is assumed that the particle moves at nonrelativistic speeds and that spectral correlations of the electromagnetic field along the particle's direction of motion are spatially invariant and/or the amplitude of the mechanical oscillator is much smaller than the spatial variations of the electromagnetic field spectral correlations. It turns out that γ is only dependent on the stochastic properties of the driving force and thus the theory also holds for the absence of a potential. Our approach for calculating γ is based on the fluctuation-dissipation theorem [25–27]. We derive the stochastic force spectrum acting on the particle and we relate it to the damping coefficient. The final expression for γ involves spectral coherence functions of the electromagnetic field. Our theory is applied to the particular situation where a particle oscillates parallel to the planar surface of a substrate.

The organization of this article is as follows. Sec. II presents the derivation of the linear-damping coefficient based on the fluctuation-dissipation theorem. In Sec. III, we apply the theory to the case of a small particle oscillating parallel to a planar interface. In Sec. IV we consider a spherical particle and we calculate and analyze the damping coefficient in the nonretarded limit for particles and substrates made of silver and glass. The analysis includes spectral properties of the damping coefficient, as well as distance dependence of the particle-surface separation and temperature. In the same section we present a discussion and comparison of the theory with the aforementioned experiments. Finally, the conclusions are presented in Sec. V.

II. THEORY

A. Equation of motion due to force fluctuations

As mentioned previously, the specific properties of the potential are irrelevant but for simplicity we consider a small particle moving in a one-dimensional harmonic potential. The potential gives rise to particle oscillation in the x direction. The particle is surrounded by vacuum and it can be placed near an arbitrary physical boundary. The particle is interacting with a thermal bath and its motion of the center-of-mass coordinate $x(t)$ is governed by the classical Langevin equation

$$m\frac{d^2}{dt^2}x(t)+\int_{-\infty}^{t}\gamma(t-t')\frac{d}{dt'}x(t')dt'+mw_o^2x(t)=F_x(t). \tag{1}$$

Here, m is the mass of the particle, $\gamma(t)$ is the damping coefficient originating from thermal electromagnetic field fluctuations, w_o is the natural frequency of the oscillator, and $F_x(t)$ is the stochastic force. We assume that $F_x(t)$ is a stationary stochastic process with zero ensemble average. If $\langle F_x(t)\rangle$ does not vanish, a variable transformation $[F_x(t)-\langle F_x(t)\rangle]$ can be applied to obtain a system driven by a force with zero average. The spectral force spectrum $S_{\mathrm{F}}(\omega)$ is given by the Wiener-Khintchine theorem as [28]

$$S_{\mathrm{F}}(\omega)=\frac{1}{2\pi}\int_{-\infty}^{\infty}\langle F_x(\tau)F_x(0)\rangle e^{i\omega\tau}d\tau, \tag{2}$$

where ω is the angular frequency. At thermal equilibrium with temperature T, the magnitude of the strength of the fluctuating force (force spectrum) is related to the friction coefficient by the fluctuation-dissipation theorem. The latter is considered in the classical limit because the motion of the macroscopic particle obeys classical mechanical laws [25,26]

$$\frac{k_{\mathrm{B}}T}{\pi}\tilde{\gamma}(\omega)=S_{\mathrm{F}}(\omega). \tag{3}$$

k_{B} is Boltzmann's constant, and $\tilde{\gamma}(\omega)$ is the Fourier transform of $\gamma(t)$ defined *only* for $t>0$. Hereafter, a tilded character denotes the Fourier transform as defined by Eq. (A2) (see Appendix A).

In the electric-dipole approximation, the force acting on a small particle moving with a velocity much less than the speed of light is [29]

$$F_x(t)=\mathbf{p}(t)\cdot\frac{\partial}{\partial x}\mathbf{E}(\mathbf{r}_o,t)+\frac{d}{dt}[\mathbf{p}(t)\times\mathbf{B}(\mathbf{r}_o,t)]\cdot\mathbf{n}_x. \tag{4}$$

Here, $\mathbf{r}_o$ is the equilibrium position of the mechanical oscillator, $\mathbf{n}_x$ is the unit vector in the x direction, $\mathbf{p}(t)$ is the electric-dipole moment of the particle, and $\mathbf{E}(\mathbf{r}_o,t)$ and $\mathbf{B}(\mathbf{r}_o,t)$ are the electric field and magnetic induction field, respectively. We omit the last term on the right-hand side of Eq. (4) because, in the Markovian approximation for the damping coefficient, this term does not contribute to the force spectrum (see Sec. II B).

B. Markovian limit for the damping coefficient

In Eq. (1), we assumed a general friction force term whose magnitude at time t depends on the particle's velocity at earlier times. We now consider that the interaction time of the thermal bath with the particle is fast compared with the particle's dynamics; thus, the change of the velocity of the particle during the interaction time is very small. The validity of the Markovian approximation can be estimated as follows. For a system with a constant damping coefficient γ_o, the characteristic time is $\tau_{\mathrm{c}}=m/\gamma_o$ (time for which the amplitude decays $1/e$ of its initial value). If the light-matter inter-

action times τ_{int} are much smaller than τ_c ($\tau_c/\tau_{\text{int}} \gg 1$), the Markovian limit is a good approximation. Assuming a spherical glass particle with a radius of 50 nm ($m \approx 10^{-18}$ kg), $\gamma_o < 10^{-12}$ kg/s (according to experiments), we find that $\tau_c > 1$ μs. Typical interaction times τ_{int} for Rayleigh scattering are much shorter than τ_c and, hence, the Markovian approximation is valid. We thus write

$$F_{\text{friction}}(t) = -\gamma_o \frac{d}{dt} x(t), \tag{5}$$

$$\gamma_o = \int_0^\infty \gamma(t)\, dt. \tag{6}$$

Evaluating Eq. (3) at $\omega = 0$ and using Eq. (6) we find that the damping constant is related to the force spectrum as

$$\frac{1}{\pi} k_B T \gamma_o = S_F(\omega = 0). \tag{7}$$

Equation (7) is the final expression that relates the linear-velocity damping coefficient to the force spectrum. To calculate γ_o, we need to solve for the force spectrum which, in turn, is defined by the electromagnetic fields due to fluctuating currents in the environment and the fluctuating dipole. Notice that, the last term on the right-hand side of Eq. (4) produces a force spectrum which is proportional to ω^2 (because of the time derivative). In the Markovian limit this term vanishes exactly because the damping constant is proportional to the force spectrum at $\omega = 0$.

C. Force spectrum

The particle's dipole moment consists of two fluctuating terms: a term ($\mathbf{p}_I$) that is induced by external fluctuating currents and a term ($\mathbf{p}_F$) due to the dipole's own random fluctuations [30]. $\mathbf{p}_I$ and $\mathbf{p}_F$ are statistically independent because the fluctuating dipole and external currents are uncorrelated. Similarly, the electric field also consists of two uncorrelated, additive terms: the field generated by the external random currents ($\mathbf{E}_F$) and the field produced by the dipole's fluctuations ($\mathbf{E}_I$). The latter interacts with the particle after it has been scattered at external boundaries [30].

To lowest approximation, the induced dipole moment is related to the external field as

$$\tilde{\mathbf{p}}_I(\omega) = \alpha(\omega) \tilde{\mathbf{E}}_F(\mathbf{r}_o, \omega), \tag{8}$$

where $\alpha(\omega)$ is the particle polarizability. $\tilde{\mathbf{E}}_F$ and $\tilde{\mathbf{p}}_I$ are *symbolic* representations of the Fourier transforms of $\mathbf{E}_F(t)$ and $\mathbf{p}_I(t)$, respectively (a rigorous mathematical formalism requires the stochastic processes to be analyzed according to the generalized theory of functions). On the other hand, the field produced by the fluctuating dipole is defined through the Green's dyadic of the system $\overleftrightarrow{\mathbf{G}}$ as (assuming a fixed equilibrium position of the dipole)

$$\tilde{\mathbf{E}}_I(\mathbf{r}, \omega) = \frac{\omega^2}{\varepsilon_o c^2} \overleftrightarrow{\mathbf{G}}(\mathbf{r}, \mathbf{r}_o, \omega) \tilde{\mathbf{p}}_F(\omega). \tag{9}$$

Here, c is the vacuum speed of light and ε_o is the vacuum electric permittivity. Considering the two terms of $\mathbf{E}$ and $\mathbf{p}$, the Fourier transform of Eq. (4) yields

$$\tilde{F}_x(\omega) = \sum_{i=1}^{3} [\tilde{p}_{Fi}(\omega) + \tilde{p}_{Ii}(\omega)] \otimes \left[\frac{\partial}{\partial x} \tilde{E}_{Fi}(\omega) + \frac{\partial}{\partial x} \tilde{E}_{Ii}(\omega) \right], \tag{10}$$

where $\otimes$ denotes convolution, and the index $i = 1,2,3$ refers to the Cartesian components x, y, z, respectively. Hereafter, a field quantity is implicitly evaluated at $\mathbf{r}_o$. For a stationary process, Eq. (2) and Eq. (10) lead to

$$\begin{aligned} \langle \tilde{F}_x^*(\omega') \tilde{F}_x(\omega) \rangle &= S_F(\omega)\, \delta(\omega - \omega') \\ &= \sum_{i,j=1}^{3} \left\langle \left[[\tilde{p}_{Fj}^*(\omega') + \tilde{p}_{Ij}^*(\omega')] \right. \right. \\ &\quad \otimes \left(\frac{\partial}{\partial x} \tilde{E}_{Fj}^*(\omega') + \frac{\partial}{\partial x} \tilde{E}_{Ij}^*(\omega') \right) \Big] \\ &\quad \times \Big[[\tilde{p}_{Fi}(\omega) + \tilde{p}_{Ii}(\omega)] \\ &\quad \left. \left. \otimes \left(\frac{\partial}{\partial x} \tilde{E}_{Fi}(\omega) + \frac{\partial}{\partial x} \tilde{E}_{Ii}(\omega) \right) \right] \right\rangle, \end{aligned} \tag{11}$$

where the asterisk * denotes the complex conjugate, and δ is the Dirac delta function. Each of the additive terms of $\langle \tilde{F}_x^*(\omega') \tilde{F}_x(\omega) \rangle$ is a fourth-order frequency-domain correlation function.

Thermal fluctuating electromagnetic fields can be thought of as arising from the superposition of a large number of radiating oscillators with a broadband spectrum. Consequently, the central-limit theorem applies and the electromagnetic field obeys Gaussian statistics. The same is true for the dipole fluctuations because of their broad thermal spectrum. Stochastic processes with Gaussian statistics have the property that a fourth-order correlation function can be expressed by a sum of pair products of second-order correlation functions. Consequently, Eq. (11) can be calculated by knowing the second-order correlation of the thermal electromagnetic fields and the electric-dipole fluctuations. At *thermal equilibrium*, the second-order correlation functions for the fluctuating electric field components (including the electric field gradient components) can be expressed in terms of the Green's tensor $G_{ij}(\mathbf{r}_o, \mathbf{r}_o', \omega)$ of the system in which the par-

ticle is embedded as [31–33]

$$\left\langle \frac{\partial^m}{\partial x'^m}\tilde{E}^*_{\mathrm{F}j}(\omega')\frac{\partial^n}{\partial x^n}\tilde{E}_{\mathrm{F}i}(\omega)\right\rangle = W^{nm}_{ij}(\omega)\,\delta(\omega-\omega'), \quad (12)$$

$$W^{nm}_{ij}(\omega)\equiv \frac{\hbar\omega^2}{c^2\pi\varepsilon_o}\Upsilon(\omega,T)\frac{\partial^m}{\partial x'^m_o}\frac{\partial^n}{\partial x^n_o} \times \mathrm{Im}[G_{ij}(\mathbf{r}_o,\mathbf{r}'_o,\omega)]\big|_{\mathbf{r}'_o=\mathbf{r}_o}. \quad (13)$$

Similarly, the second-order correlation function of dipole fluctuations takes on the form [31–33]

$$\langle p^*_{\mathrm{F}i}(\omega)p_{\mathrm{F}j}(\omega)\rangle = P(\omega)\tilde{\delta}_{ij}\delta(\omega-\omega'), \quad (14)$$

$$P(\omega)\equiv\frac{\hbar}{\pi}\Upsilon(\omega,T)\mathrm{Im}[\alpha(\omega)]. \quad (15)$$

Here, $\hbar$ is the reduced Planck's constant, $\tilde{\delta}_{ij}$ is the Kronecker tensor, $\mathrm{Im}[\cdots]$ denotes imaginary part, $(n,m=0,1)$ with $\partial^0/\partial x^0$ representing the unit operator, and $\Upsilon(\omega,T)$ is defined as

$$\Upsilon(\omega,T)=\frac{1}{2}\left(1+\coth\left[\frac{\hbar\omega}{2k_{\mathrm{B}}T}\right]\right). \quad (16)$$

Equations (12), (13), (14), and (15) follow from the fluctuation-dissipation theorem applied to the density current $\mathbf{j}$—i.e., $\langle\tilde{j}^*_n(\mathbf{r}',\omega)\tilde{j}_m(\mathbf{r},\omega)\rangle\propto\mathrm{Im}[\epsilon(\mathbf{r},\omega)]\delta(\mathbf{r}-\mathbf{r}')\delta(\omega-\omega')\times\tilde{\delta}_{mn}$ with m,n denoting any Cartesian vector component, and $\epsilon(\mathbf{r},\omega)$ being the dielectric constant [31–33]. Absorption and emission of electromagnetic energy in a system occur over a spectrum of positive and negative frequencies. The factor $\Upsilon(\omega,T)$ weights the thermal occurrence of these absorption and emission events as a function of temperature T and angular frequency ω [33]. It has to be emphasized that we assign the full quantum properties to the exterior currents and to the dipole fluctuations, whereas the motion of the particle is considered in the classical statistical limit [cf. Eq. (3)]. In summary, the results derived in this section allow us to calculate the force spectrum acting on a polarizable particle in an arbitrary system in thermal equilibrium.

III. FORCE SPECTRUM NEAR A SUBSTRATE WITH A PLANE SURFACE

We consider a half-space $(z<0)$ filled with a material having a local complex dielectric constant $\epsilon_2(\omega)$. A polarizable particle is placed at a fixed vertical distance z_o from the surface and it moves in a harmonic potential parallel to the surface (x direction) (see Fig. 1).

It turns out that the total force spectrum $S_{\mathrm{F}}(\omega)$ given by Eq. (11) can be expressed as a sum of four terms as

$$S_{\mathrm{F}}(\omega)=S_{\mathrm{A}}(\omega)+S_{\mathrm{B}}(\omega)+S_{\mathrm{C}}(\omega)+S_{\mathrm{D}}(\omega). \quad (17)$$

Each of these terms has a different physical origin which will be discussed in the following subsections. In the Markovian limit, the damping coefficient γ_o is related to $S_{\mathrm{F}}(\omega=0)$ through Eq. (7), and by using Eq. (17), γ_o can be expressed as the sum of four terms as

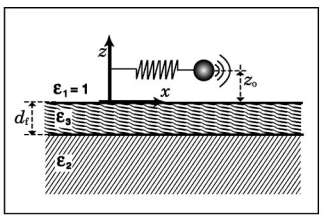

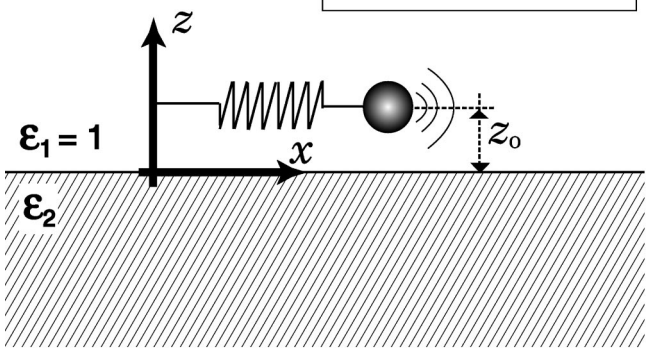

FIG. 1. A particle in vacuum ($\epsilon_1=1$) oscillates parallel to a substrate with a planar surface and a dielectric function $\epsilon_2(\omega)$. In the inset, the particle's environment is modified by adding a layer with thickness d_{f} and dielectric constant $\epsilon_3(\omega)$.

$$\gamma_o=\sum_{l=1}^{4}\gamma_{lo}, \quad (18)$$

$$\frac{k_{\mathrm{B}}T}{\pi}\gamma_{lo}=S_l(\omega=0). \quad (19)$$

Here, $l=1,2,3,4$ refers to letters A,B,C,D, respectively.

A. Interaction between p_{I} and E_{F}

The spectrum $S_{\mathrm{A}}(\omega)$ is related to the correlation of the induced dipole with the gradient of the external thermal field according to

$$S_{\mathrm{A}}(\omega)\,\delta(\omega-\omega')=\sum_{i,j=1}^{3}\left\langle\left(\tilde{p}^*_{\mathrm{I}j}(\omega')\otimes\frac{\partial}{\partial x}\tilde{E}^*_{\mathrm{F}j}(\omega')\right)\times\left(\tilde{p}_{\mathrm{I}i}(\omega)\otimes\frac{\partial}{\partial x}\tilde{E}_{\mathrm{F}i}(\omega)\right)\right\rangle. \quad (20)$$

We substitute Eq. (8) into Eq. (20) and expand the fourth-order correlation functions of Eq. (20) into second-order correlation functions by using Eq. (A3) (cf. Appendix A). Then, we express the second-order correlation functions by the Green's dyadics of the half-space [34]. The spectrum $S_{\mathrm{A}}(\omega)$ turns out to be

$$S_{\mathrm{A}}(\omega)=\sum_{i=1}^{3}|\alpha(\omega)|^2 W_{ii}^{00}(\omega)\otimes W_{ii}^{11}(\omega)+\alpha^*(\omega)W_{zx}^{10}(\omega)\otimes\alpha(\omega)W_{zx}^{01}(\omega)+\alpha^*(\omega)W_{xz}^{10}(\omega)\otimes\alpha(\omega)W_{xz}^{01}(\omega). \tag{21}$$

We evaluate the spectrum $S_{\mathrm{A}}(\omega)$ at $\omega=0$ to obtain the damping coefficient $\gamma_{\mathrm{A}o}$ [see Eq. (19)]. The convolution integral of Eq. (21) runs from $-\infty$ to ∞. However, the convolution for $S_{\mathrm{A}}(\omega=0)$ can be expressed by an integral running from 0 to ∞ by using the frequency-inversion properties of $\alpha(\omega)$ and the explicit form of $W_{ij}^{nm}(\omega)$ for a planar interface. Therefore, Eq. (19) for $S_{\mathrm{A}}(\omega=0)$ can be expressed as

$$\frac{k_{\mathrm{B}}T}{\pi}\gamma_{\mathrm{A}o}=S_{\mathrm{A}}(0)=\int_0^\infty 2\,\eta(\omega,T)\times\{|\alpha(\omega)|^2[f_{\mathrm{A}1}(z_o,\omega)g_{\mathrm{A}1}(z_o,\omega)+f_{\mathrm{A}2}(z_o,\omega)g_{\mathrm{A}2}(z_o,\omega)]-2\,\mathrm{Re}[\alpha(\omega)^2]\times[f_{\mathrm{A}3}(z_o,\omega)]^2\}d\omega, \tag{22}$$

where

$$\eta(\omega,T)\equiv-\Upsilon(-\omega,T)\Upsilon(\omega,T)=[1/(\mathrm{e}^{\hbar\omega/k_{\mathrm{B}}T}-1)][1+1/(\mathrm{e}^{\hbar\omega/k_{\mathrm{B}}T}-1)], \tag{23}$$

with $\mathrm{Re}[\cdots]$ denoting the real part. Explicit expressions for $f_{\mathrm{A}1}$, $f_{\mathrm{A}2}$, $f_{\mathrm{A}3}$, $g_{\mathrm{A}1}$, and $g_{\mathrm{A}2}$ are presented in Appendix B. $f_{\mathrm{A}1}$ and $f_{\mathrm{A}2}$ are related to the spectral correlation of the Cartesian components of the electric field while $g_{\mathrm{A}1}$ and $g_{\mathrm{A}2}$ represent the spectral correlation of the partial derivative with respect to the x coordinate of the Cartesian components. $f_{\mathrm{A}3}$ is related to the cross-term spectral correlation function between the x and z electric field components and the partial derivative with respect to x of those electric field components. The factor $\eta(\omega,T)$ accounts for the strength of thermal excitations at frequency ω. $f_{\mathrm{A}i}$ and $g_{\mathrm{A}j}$ ($i=1,2,3$, $j=1,2$) contain integral expressions of the form I_{nm}^{ζ} defined in Appendix B. The integral I_{nm}^{ζ} has one dimensionless quadrature q, and the integration interval can be split into two subintervals; namely, $0<q<1$ and $q>1$. For $0<q<1$, the argument of the exponential function in the integrand is imaginary giving rise to propagating waves. On the other hand, for $q>1$ the argument of the exponential function becomes real and negative (evanescent waves); thus, the integrand decays as q is increased. The decay rate is determined by the magnitude of $\omega z_o/c$.

The interaction of the particle with evanescent waves ($\omega z_o/c\ll 1$)—that is, the near-field zone—is dominated by terms I_{nm}^{p} (p polarization) which allows us to drop s-polarized terms as well as the contribution of propagating waves ($0<q<1$). $I_{nm}^{p}(z_o,\omega)$ increases with increasing value of $n+m$. Depending on the intrinsic material properties of the half-space, I_{nm}^{p} can exhibit resonances (polaritons) determined through the Fresnel reflection coefficient for p polarization. The integral I_{nm}^{ζ} vanishes in both subintervals as $\omega z_o/c\to\infty$. In this limit only free-space terms survive; that is, friction exists even in absence of the interface. The free-space limit is discussed in Appendix G. Notice that the here derived damping coefficient $\gamma_{\mathrm{A}o}$ is determined by the factors $|\alpha(\omega)|^2$ and $\mathrm{Re}[\alpha(\omega)^2]$.

B. Interaction between p_{F} and E_{F}

The spectrum $S_{\mathrm{B}}(\omega)$ originates from the correlation of the particle's dipole fluctuations and the gradient of the external fluctuating field according to

$$S_{\mathrm{B}}(\omega)\,\delta(\omega-\omega')=\sum_{i,j=1}^{3}\left\langle\left(\tilde{p}_{\mathrm{F}j}^{*}(\omega')\otimes\frac{\partial}{\partial x}\tilde{E}_{\mathrm{F}j}^{*}(\omega')\right)\times\left(\tilde{p}_{\mathrm{F}i}(\omega)\otimes\frac{\partial}{\partial x}\tilde{E}_{\mathrm{F}i}(\omega)\right)\right\rangle. \tag{24}$$

Here, the fluctuations of dipole and field are *statistically independent*. The fourth-order correlation can be split into pair products of second-order correlation functions as in Eq. (A3). Furthermore, second-order correlation functions with two statistically independent variables can be eliminated. Then, the spectrum $S_{\mathrm{B}}(\omega)$ becomes

$$S_{\mathrm{B}}(\omega)=P(\omega)\otimes[W_{xx}^{11}(\omega)+W_{yy}^{11}(\omega)+W_{zz}^{11}(\omega)]. \tag{25}$$

As before, we evaluate the spectrum $S_{\mathrm{B}}(\omega)$ at $\omega=0$ to obtain $\gamma_{\mathrm{B}o}$ [see Eq. (19)]. Also, by using the frequency-inversion properties of $P(\omega)$ and $W_{ii}^{11}(\omega)$ the convolution can be reduced to positive frequencies only and $\gamma_{\mathrm{B}o}$ becomes

$$\frac{k_{\mathrm{B}}T}{\pi}\gamma_{\mathrm{B}o}=S_{\mathrm{B}}(0)=2\int_0^\infty\eta(\omega,T)\frac{\hbar}{\pi}\mathrm{Im}[\alpha(\omega)]g_{\mathrm{B}}(\omega)d\omega. \tag{26}$$

The full expression of g_{B} is given in Appendix C. Similar to $g_{\mathrm{A}1}$, g_{B} is related to correlations of fluctuating field gradients. Also, g_{B} consists of integral functions of the type I_{nm}^{ζ} and, consequently, the conclusions from the previous section apply here as well. Similar to the case of $\gamma_{\mathrm{A}o}$, the damping coefficient $\gamma_{\mathrm{B}o}$ does *not* vanish in free space. This limit is discussed in Appendix G. In the nonretarded limit ($\omega z_o/c\ll 1$), Eq. (26) reduces to the result derived in Ref. [14] which is further analyzed in Ref. [16] for the case of metallic particles and substrates. The fact that previous results are recovered by the here presented theory validates our approach.

C. Interaction between p_{I} and E_{I}

$S_{\mathrm{C}}(\omega)$ is related to the fourth-order correlation of the induced electric-dipole and the induced electromagnetic fluctuations. The spectrum $S_{\mathrm{C}}(\omega)$ is given by the expression

$$S_{\mathrm{C}}(\omega)\,\delta(\omega-\omega')=\sum_{i,j=1}^{3}\left\langle\left(\tilde{p}_{\mathrm{I}j}^{*}(\omega')\otimes\frac{\partial}{\partial x}\tilde{E}_{\mathrm{I}j}^{*}(\omega')\right)\times\left(\tilde{p}_{\mathrm{I}i}(\omega)\otimes\frac{\partial}{\partial x}\tilde{E}_{\mathrm{I}i}(\omega)\right)\right\rangle. \tag{27}$$

Here, the induced dipole and the induced field are *statistically independent*. We substitute Eqs. (8) and (9) into Eq. (27). After separating the fourth-order correlation functions into pairs of second-order correlations we obtain

$$S_{\mathrm{C}}(\omega)=|\alpha(\omega)|^2[W_{xx}^{00}(\omega)+W_{zz}^{00}(\omega)] \otimes \frac{\omega^4}{c^4\varepsilon_o^2}P(\omega)\left|\frac{\partial}{\partial x}G_{13}(\mathbf{r},\mathbf{r}_o,\omega)|_{\mathbf{r}=\mathbf{r}_o}\right|^2. \quad (28)$$

To obtain $\gamma_{\mathrm{C}o}$, the spectrum $S_{\mathrm{C}}(\omega)$ is evaluated at $\omega=0$. Using the frequency-inversion properties of the different terms in Eq. (28) we find

$$\frac{k_{\mathrm{B}}T}{\pi}\gamma_{\mathrm{C}o}=S_{\mathrm{C}}(0)=2\int_0^\infty \eta(\omega,T)|\alpha(\omega)|^2 f_{\mathrm{C}}(z_o,\omega) \times \mathrm{Im}[\alpha(\omega)]g_{\mathrm{C}}(z_o,\omega)d\omega. \quad (29)$$

Explicit expressions for f_{C} and g_{C} are given in Appendix D. f_{C} is related to correlations of fluctuating fields whereas g_{C} originates from correlations of induced field gradients that are induced by dipole fluctuations. Also, f_{C} and g_{C} contain integral functions of the type I_{nm}^{ζ}. Furthermore, g_{B} contains only terms that are due to *p*-polarized fields. Thus, as $\omega z_o/c\to\infty$ the damping coefficient $\gamma_{\mathrm{C}o}$ vanishes. This can be understood from the fact that the field generated by the dipole fluctuations does not interact with the particle if there are no scatterers in the environment.

D. Interaction between p_{F} and E_{I}

The spectrum $S_{\mathrm{D}}(\omega)$ refers to the fourth-order correlation of dipole fluctuations and the gradients of the induced electromagnetic field. It is given by

$$S_{\mathrm{D}}(\omega)\delta(\omega-\omega')=\sum_{i,j=1}^{3}\left\langle\left(\tilde{p}_{\mathrm{F}j}^{*}(\omega')\otimes\frac{\partial}{\partial x}\tilde{E}_{\mathrm{I}j}^{*}(\omega')\right)\times\left(\tilde{p}_{\mathrm{F}i}(\omega)\otimes\frac{\partial}{\partial x}\tilde{E}_{\mathrm{I}i}(\omega)\right)\right\rangle. \quad (30)$$

By substituting Eq. (9) and then repeating the same procedure for expressing fourth-order correlations functions in terms of second-order correlation functions yields

$$S_{\mathrm{D}}(\omega)=2P(\omega)\otimes\frac{\omega^4}{c^4\varepsilon_o^2}P(\omega)\left|\frac{\partial}{\partial x}G_{13}(\mathbf{r},\mathbf{r}_o,\omega)|_{\mathbf{r}=\mathbf{r}_o}\right|^2 + \left(\frac{\omega^2}{c^2\varepsilon_o}P(\omega)\frac{\partial}{\partial x}G_{13}(\mathbf{r},\mathbf{r}_o,\omega)|_{\mathbf{r}=\mathbf{r}_o}\right) \otimes\left(\frac{\omega^2}{c^2\varepsilon_o}P(\omega)\frac{\partial}{\partial x}G_{31}^{*}(\mathbf{r},\mathbf{r}_o,\omega)|_{\mathbf{r}=\mathbf{r}_o}\right) + \left(\frac{\omega^2}{c^2\varepsilon_o}P(\omega)\frac{\partial}{\partial x}G_{31}(\mathbf{r},\mathbf{r}_o,\omega)|_{\mathbf{r}=\mathbf{r}_o}\right) \otimes\left(\frac{\omega^2}{c^2\varepsilon_o}P(\omega)\frac{\partial}{\partial x}G_{13}^{*}(\mathbf{r},\mathbf{r}_o,\omega)|_{\mathbf{r}=\mathbf{r}_o}\right). \quad (31)$$

Evaluating the spectrum $S_{\mathrm{D}}(\omega)$ at $\omega=0$ and reducing the convolution integral to positive frequencies leads to

$$\frac{1}{\pi}\frac{k_{\mathrm{B}}}{T}\gamma_{\mathrm{D}o}=\int_0^\infty \eta(\omega,T)\mathrm{Im}^2[\alpha(\omega)]f_{\mathrm{D}}(z_o,\omega)d\omega. \quad (32)$$

The explicit expression for f_{D} is given in Appendix E. It is made of purely *p*-polarized fields. Consequently, in the limit $\omega z_o/c\to\infty$ the damping coefficient $\gamma_{\mathrm{D}o}$ vanishes.

E. Total damping coefficient

Equations (22), (26), (29), and (32) are the final expressions for calculating the total linear-velocity damping coefficient γ_o according to Eq. (19). For temperature $T=0$ K, γ_o vanishes because of $\eta(\omega,T=0)=0$. This can be explained from the fact that zero-point fluctuations are invariant under the Lorentz transformation [35]. In the following section, we analyze the properties of the damping coefficients $\gamma_{\mathrm{A}o}$ and $\gamma_{\mathrm{B}o}$. $\gamma_{\mathrm{C}o}$ and $\gamma_{\mathrm{D}o}$ are omitted because their contribution is negligible (see discussion in Appendix F).

IV. LINEAR DAMPING COEFFICIENT FOR A SPHERICAL PARTICLE

We consider a spherical particle of radius *a* with polarizability

$$\alpha(\omega)=4\pi\varepsilon_o a^3\frac{\epsilon_{\mathrm{p}}(\omega)-1}{\epsilon_{\mathrm{p}}(\omega)+2}, \quad (33)$$

where $\epsilon_{\mathrm{p}}(\omega)$ is the dielectric constant of the particle. In the limit $\omega z_o/c\ll 1$, the contribution of *p*-polarized evanescent waves in Eqs. (22) and (26) dominates and the contribution of free space terms and *s*-polarized terms can be discarded. In this limit, $r_{12}^{p}\approx[\epsilon_2(\omega)-1]/[\epsilon_2(\omega)+1]$ and (cf. Appendix B)

$$I_{nm}^{p}(z_o,\omega)\approx\frac{\epsilon_2(\omega)-1}{\epsilon_2(\omega)+1}\mathrm{i}^m\int_0^\infty q^{n+m}e^{-2\omega z_o q/c}dq. \quad (34)$$

As we will discuss later on, Eq. (34) is of central importance because it defines the distance dependence of the damping coefficient and its dependence on the substrate properties. For the cases considered in this section, the condition $\omega z_o/c\ll 1$ is fulfilled over the entire frequency spectrum for all distances and for all considered temperatures.

We consider particles and substrates made of two types of materials: silver (Ag), a noble metal, and glass (SiO_2), a polar dielectric. The damping coefficient is calculated for any combination of these materials. Glass and silver possess

opposite dielectric properties and both materials exhibit surface modes. The surface modes of silver (surface plasmon polaritons) exist in the visible spectrum, whereas the surface modes of glass (surface phonon polaritons) are in the infrared.

In the angular frequency range 0.19×10^{15}–15×10^{18} Hz the dielectric constant of silver is obtained by using a linear interpolation (on a log-log scale) of the data in Ref. [36]. The Drude model is used to extrapolate the data below 0.19×10^{15} Hz. The Drude model parameters for silver are $\omega_{\rm pl}=13.6\times10^{15}$ Hz and $\Gamma=27.3\times10^{12}$ Hz ($\omega_{\rm pl}$ is the plasma frequency, and Γ is the damping factor) [37]. The same interpolation method is applied to derive the complex dielectric constant of glass in the frequency ranges of 0.75–2.6×10^{12} Hz and 3.7×10^{12}–1.9×10^{17} Hz using the data of Refs. [38,39]. The dielectric constant in the frequency gap between the two data sets is calculated by using a linear log-log interpolation procedure. In the frequency range below 0.75×10^{12} Hz, the real part of the dielectric constant of glass is nearly uniform ($\mathrm{Re}[\epsilon_2(\omega)]\approx3.82$), and the imaginary part is calculated according to

$$\mathrm{Im}[\epsilon_2(\omega)]=\frac{1}{\varrho_{\rm g}\varepsilon_o\omega}, \tag{35}$$

where $\varrho_{\rm g}$ is the dc resistivity of SiO_2. This equation determines the *conductive* contribution to the glass dielectric constant. It accounts for defects and the finite thermal occupation of the conduction band. The exact value of $\varrho_{\rm g}$ varies with temperature, but for simplicity we assume a constant value of $\varrho_{\rm g}=3\times10^{8}\ \Omega$ m (room temperature) [40]. As will be discussed later, the damping constant of the oscillating particle is almost entirely defined by Eq. (35) if the particle and half-space are made of glass.

A. Damping coefficient γ_{Ao}

By substituting Eq. (33) into Eq. (22) and by using approximation (34) in Eqs. (B1)–(B5), the damping coefficient $\gamma_{\rm A}$ in the nonretarded limit is found to be

$$\gamma_{{\rm A}o}=\frac{9\hbar^2}{32\pi k_{\rm B}T}\frac{a^6}{z_o^8}\int_0^\infty\left(|\xi(\omega)|^2-\frac{1}{2}\mathrm{Re}[\xi^2(\omega)]\right)\times\mathrm{Im}^2\left[\frac{\epsilon_2(\omega)-1}{\epsilon_2(\omega)+1}\right]\eta(\omega,T)d\omega. \tag{36}$$

Here, $\xi(\omega)\equiv\alpha(\omega)/(4\pi\varepsilon_o a^3)$. Notice that $\gamma_{{\rm A}o}$ is directly proportional to the factor

$$f_{\rm A}=\frac{a^6}{z_o^8}, \tag{37}$$

i.e., the square of the particle volume and the inverse eight power of the separation between the particle center and the surface.

It is important to stress that in the low-frequency region,

$$\mathrm{Im}[(\epsilon_2(\omega)-1)/(\epsilon_2(\omega)+1)]\approx2\varepsilon_o\omega/\sigma, \tag{38}$$

$$|\xi(\omega)|^2=\mathrm{Re}[\xi^2(\omega)]\approx1. \tag{39}$$

Here σ is the conductivity. The frequency range in which these approximations are valid depends on the type of material. For glass, this frequency range is $\Delta\omega\approx20$ Hz whereas for silver it is $\Delta\omega\approx10^{15}$ Hz. The conductivity of silver is determined as $\sigma=\varepsilon_o\omega_{\rm pl}^2/\Gamma$, whereas the glass conductivity is $\sigma=1/\varrho_{\rm g}$.

Let us define the threshold frequency as $\Omega_{\rm T}=k_{\rm B}T/\hbar=0.13\times10^{12}\ T(\mathrm{K})$ Hz. Then, for frequencies $\omega<\sim0.4\Omega_{\rm T}$ we can use the approximation $\eta(\omega,T)\approx[k_{\rm B}T/(\hbar\omega)]^2$. The low-frequency contribution to the damping coefficient $\gamma_{{\rm A}o}$ in Eq. (36) can now be written as

$$\gamma_{{\rm A}o}^{\rm low}=\frac{9}{16\pi}\frac{a^6}{z_o^8}\frac{\varepsilon_o^2}{\sigma_{\rm s}^2}k_{\rm B}T\,\mathrm{Min}[\Delta\omega_{\rm s},\Delta\omega_{\rm p},0.4\Omega_T], \tag{40}$$

where $\mathrm{Min}[\cdots]$ denotes the minimum of the values in the brackets and the subscripts ''s'' and ''p'' refer to surface and particle, respectively. $\gamma_{{\rm A}o}^{\rm low}$ is a valid approximation in the frequency range $0<\omega<\mathrm{Min}[\Delta\omega_{\rm s},\Delta\omega_{\rm p},0.4\Omega_T]$.

In general, $\gamma_{{\rm A}o}$ depends on the pair-correlation products of the sort $\langle\tilde{E}_{\rm F}^*\,\tilde{E}_{\rm F}\rangle\langle\partial_x\tilde{E}_{\rm F}^*\,\partial_x\tilde{E}_{\rm F}\rangle$ and $\langle\tilde{E}_{\rm F}^*\,\partial_x\tilde{E}_{\rm F}\rangle\langle\tilde{E}_{\rm F}^*\,\partial_x\tilde{E}_{\rm F}\rangle$. In the low-frequency regime, the distance dependence (z_o^{-8}) of $\gamma_{{\rm A}o}^{\rm low}$ originates from Eq. (34) and together with Eq. (38) gives the substrate conductivity dependence ($\sigma_{\rm s}^{-2}$) of $\gamma_{{\rm A}o}^{\rm low}$, since $\langle\tilde{E}_{\rm F}^*\tilde{E}_{\rm F}\rangle\propto\sigma_{\rm s}^{-1}z_o^{-3}$, $\langle\partial_x\tilde{E}_{\rm F}^*\partial_x\tilde{E}_{\rm F}\rangle\propto\sigma_{\rm s}^{-1}z_o^{-5}$, and $\langle\tilde{E}_{\rm F}^*\,\partial_x\tilde{E}_{\rm F}\rangle\propto\sigma_{\rm s}^{-1}z_o^{-4}$. The damping coeffient in this regime depends *only* on the conductive properties of the substrate and *not* on the particle properties.

The normalized integrand of Eq. (36)—i.e., the normalized spectral density of the damping coefficient—is plotted in Fig. 2 as a function of the angular frequency ω for the temperatures $T=3$ K, 30 K, 300 K. The curves depend on the material properties of particle and substrate. We assume that the dielectric constants $\epsilon_2(\omega)$ of glass and silver do not vary with temperature (lack of data for low temperature). Notice that the scales in the figures for the glass substrate differ by many orders of magnitude from the scales obtained for silver substrates. In the case in which the particle and substrate are made of silver [Fig. 2(a)], the normalized spectrum remains flat up to a certain cutoff frequency. The peak in the curve for $T=300$ K is an artifact due to the weak mismatch between the Drude model and the data from Ref. [36]. This mismatch does not significantly contribute to the integrated value of the damping constant. The cutoff frequency corresponds approximately to $0.4\Omega_{\rm T}$ and depends linearly on the temperature T. Below the cutoff frequency, the damping coefficient is perfectly approximated by $\gamma_{{\rm A}o}^{\rm low}$ in Eq. (40). In the case of a silver substrate and a glass particle [Fig. 2(b)], the spectrum is uniform in two separate intervals with the exception of the situation $T=300$ K in which resonant peaks appear. These peaks are due to thermally excited surface polaritons of the glass particle at infrared frequencies. At $T=300$ K, the temperature is not high enough to thermally excite surface plasmons in the visible spectrum. The transition between the two uniform spectral intervals

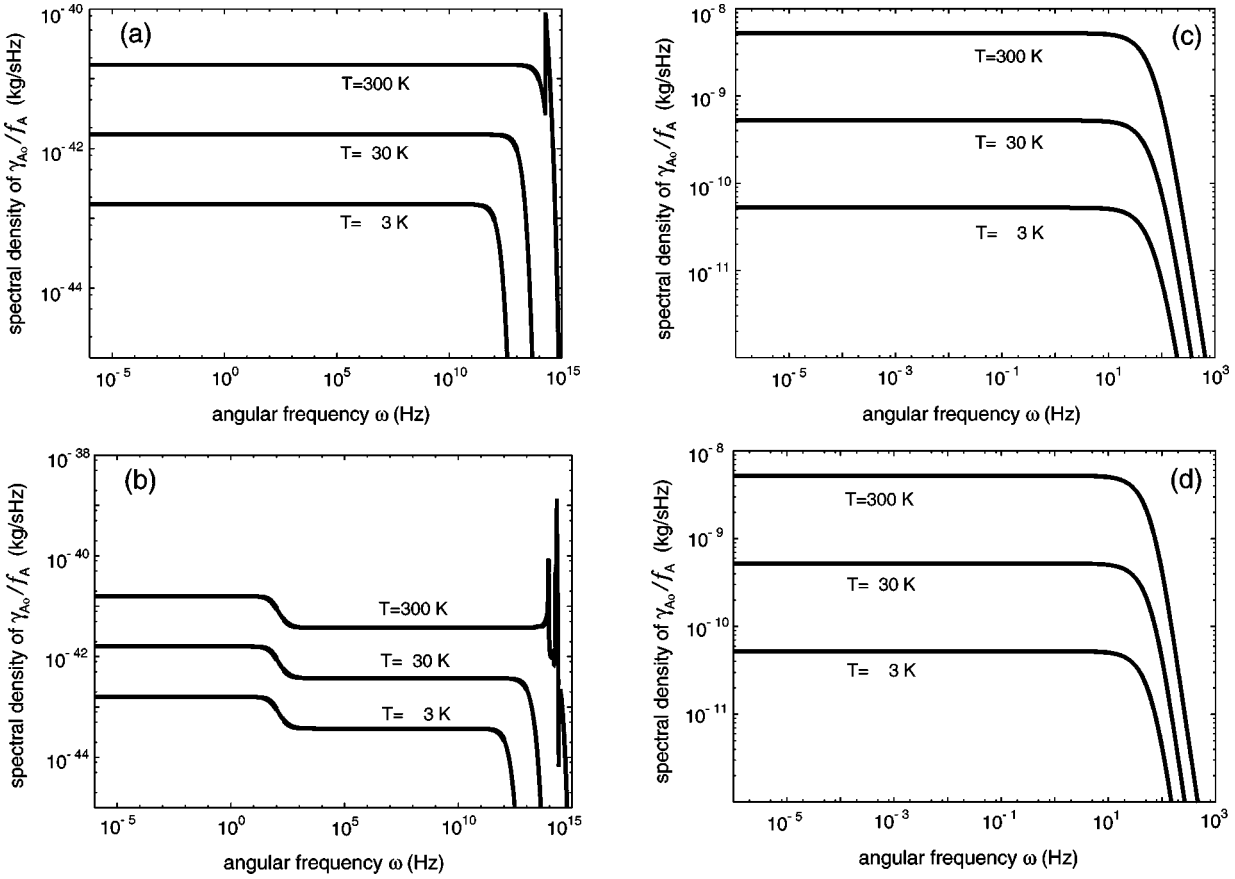

FIG. 2. Normalized spectral density of the damping coefficient γ_{Ao}/f_A as a function of the angular frequency ω [integrand of Eq. (36)] for temperatures $T=3$ K, 30 K, 300 K. $f_A=a^6/z_o^8$ where a and z_o are defined in nanometers. (a) Substrate and particle: Ag; (b) substrate: Ag, particle: SiO_2; (c) substrate: SiO_2, particle: Ag; (d) particle and substrate: SiO_2.

starts at $\Delta\omega_p \approx 20$ Hz. For temperatures $T=3$ K and 30 K, the damping coefficient is determined by frequencies smaller than $\Delta\omega_p$. However, for $T=300$ K, the largest contribution is due to the surface polariton peaks of the glass particle. In the remaining two figures, Figs. 2(c) and 2(d), the substrate is made of glass. For the silver particle the cutoff frequency turns out to be 50 Hz and for the glass particle 44 Hz, independent of temperature. The two curves are almost identical. Consequently, the integrated damping constant γ_{Ao} is independent of the particle material if a glass substrate is considered. In this case, γ_{Ao} is almost entirely determined by frequencies smaller than 100 Hz and Eq. (40) becomes an excellent approximation for $\mathrm{Min}[\Delta\omega_s,\Delta\omega_p,0.4\Omega_T]=\Delta\omega_s$. The normalized damping coefficient γ_{Ao}/f_A corresponds to the area under the spectral curves. Numerical integration renders the values listed in Table I. The normalization constant is $f_A=a^6/z_o^8$, where a and z_o are given in nanometers. The magnitude of the damping coefficient is largely determined by the material of the semi-infinite substrate. The particle properties have only a minor effect. At first glance, the difference of 19 orders of magnitude between the glass and silver substrate is very surprising. However, it can be explained by the following physical picture. The fluctuating currents in particle and substrate generate a fluctuating electromagnetic field. This field polarizes the particle and induces an electric dipole with a corresponding image dipole beneath the surface of the substrate. The motion of the particle gives rise to motion of the image dipole and hence to a current beneath the surface. The Joule losses associated with this image current become larger with increasing resistivity of the substrate. As a consequence, the damping coefficient increases, too. From Eq. (40), it is noticed that the damping coefficient is directly proportional to the *square* of the resistivity of the *substrate* and to the frequency bandwidth $\mathrm{Min}[\Delta\omega_s,\Delta\omega_p,0.4\Omega_T]$ (if γ_o^{low} approximates γ_o). Since the ratios of the resistivities and bandwidths of glass and silver are about 10^{16} and 10^{-11}, respectively, the resulting damping coefficients differ by 18 orders of magnitude which is in

TABLE I. Normalized damping coefficient γ_{Ao}/f_A for a spherical particle calculated from Eq. (36) for several temperatures ($T=3$ K, 30 K, 300 K). $f_A=a^6/z_o^8$ where a and z_o are defined in nanometers.

Substrate	Particle	γ_{Ao}/f_A (kg/s)		
		3 K	30 K	300 K
Silver	Silver	2.05×10^{-31}	2.05×10^{-29}	6.31×10^{-27}
Silver	Glass	4.82×10^{-32}	4.87×10^{-30}	1.07×10^{-26}
Glass	Silver	3.21×10^{-09}	3.21×10^{-08}	3.21×10^{-07}
Glass	Glass	2.71×10^{-09}	2.71×10^{-08}	2.71×10^{-07}

qualitative agreement with the calculated values. In the limit of $\varrho \to \infty$ the damping coefficient $\gamma_A \to \infty$, since in Eq. (40) the bandwith is proportional to $1/\varrho$ and the remaining factor to ϱ^2. Physically, more work is needed to move the induced dipole beneath the surface as ϱ increases and, consequently, the damping coefficient becomes larger. In the limit of a perfect dielectric ($\varrho \to \infty$), the induced dipole cannot be displaced and damping becomes infinitely strong. On the one hand, it is surprising to find this result for a perfect (lossless) dielectric since there is no intrinsic dissipation. On the other hand, a lossless dielectric does not exist from the point of view of causality (Kramers-Kronig relations) and the fluctuation-dissipation theorem (fluctuations imply dissipation).

B. Damping coefficient γ_{Bo}

By substituting Eq. (33) into Eq. (26) and using the approximation (34) for the integrals in g_B, the damping coefficient γ_B in the nonretarded limit ($\omega z_o/d \ll 1$) turns out to be

$$\gamma_{Bo} = \frac{3\hbar^2}{2\pi k_B T} \frac{a^3}{z_o^5} \int_0^\infty \mathrm{Im}\left[\frac{\epsilon_2(\omega)-1}{\epsilon_2(\omega)+1}\right] \mathrm{Im}[\xi(\omega)]\, \eta(\omega,T)\, d\omega. \tag{41}$$

Here, γ_{Bo} is directly proportional to the factor

$$f_B = \frac{a^3}{z_o^5}, \tag{42}$$

i.e., the particle volume and inverse fifth power of the separation between the particle center and surface. Equation (41) is identical to the result derived in Ref. [14] where it is analyzed for metallic substrates and particles.

In the low-frequency region we can approximate $\mathrm{Im}[\xi(\omega)] \approx 3\varepsilon_o \omega/\sigma_p$. As in the previous section, the frequency interval in which this approximation is valid depends on the material properties. The low-frequency contribution to the damping coefficient γ_{Bo} in Eq. (41) can be written as

$$\gamma_{Bo}^{\mathrm{low}} = \frac{9}{\pi} \frac{a^3}{z_o^5} \frac{\varepsilon_o^2}{\sigma_s \sigma_p} k_B T\, \mathrm{Min}[\Delta\omega_s, \Delta\omega_p, 0.4\Omega_T]. \tag{43}$$

$\gamma_{Bo}^{\mathrm{low}}$ is a valid approximation in the frequency range $0 < \omega < \mathrm{Min}[\Delta\omega_s, \Delta\omega_p, 0.4\Omega_T]$. In general, γ_{Bo} depends on the pair-correlation products of the sort $\langle \tilde{p}_F^*\, \tilde{p}_F \rangle \langle \partial_x \tilde{E}_F^*\, \partial_x \tilde{E}_F \rangle$. In the low-frequency regime, the distance and substrate conductivity dependence of $\gamma_{Bo}^{\mathrm{low}}$ is determined by the aforementioned result $\langle \partial_x \tilde{E}_F^* \partial_x \tilde{E}_F \rangle \propto \sigma_s^{-1} z_o^{-5}$ [cf. Eq. (34)]. In contrast to $\gamma_{Ao}^{\mathrm{low}}$, $\gamma_{Bo}^{\mathrm{low}}$ depends on the conductive properties of the particle, since $\langle \tilde{p}_F^*\, \tilde{p}_F \rangle \propto \sigma_p^{-1}$.

The normalized spectral density of the damping coefficient γ_{Bo} with respect to f_B is plotted in Fig. 3 as a function of the angular frequency ω for the temperatures $T = 3$ K, 30 K, 300 K. The curves depend on the material properties of the particle and substrate. As shown in Fig. 3, the normalized spectra of the damping coefficient are flat for all combinations of particle/substrate materials and for all considered temperatures. Consequently, the damping coefficient is correctly approximated by $\gamma_{Bo}^{\mathrm{low}}$. In the case where the particle and substrate are made of silver, the cutoff frequency of the flat spectrum is approximately $0.4\Omega_T$ and depends linearly on the temperature T [see Fig. 3(a)]. The peak in the curve for $T = 300$ K is the same artifact as in Fig. 2(a). When the materials of the particle and substrate are different (silver/glass) the cutoff frequency turns out to be independent of temperature and takes on a value of 65 Hz and 78 Hz for the plots in Figs. 3(b) and 3(c), respectively. In these cases, the damping coefficient is well described by $\gamma_{Bo}^{\mathrm{low}}$ and is limited by $\Delta\omega_s$ (substrate) or $\Delta\omega_p$ (glass). Finally, Fig. 3(d) shows the situation for a particle and substrate both made of glass. The flat spectra are limited by $\Delta\omega_{s,p}$ of glass. In this case, the cutoff frequency is independent of temperature and the damping coefficient γ_{Bo} becomes linearly dependent on T [see Eq. (43)].

The normalized damping coefficients γ_{Bo}/f_B (area under the spectral curves) obtained from numerical integration of the spectral curves are listed in Table II. The values of a and z_o are given in nanometers. It turns out that the damping coefficient for the particle and substrate both made of glass is many orders of magnitude stronger than the damping constant in any other case. This can be explained by the fact that $\gamma_{Bo}^{\mathrm{low}}$ is inversely proportional to the product of the conductivities of the particle and substrate. Thus, the presence of a silver material in the system drastically lowers the damping because of silver's high conductivity.

Similar to the previous discussion for γ_{oA}, the physical origin for the damping coefficient γ_{oB} is the resistivity acting on the image dipole. However, in the present case it is the image of the self-fluctuating dipole and not of the induced dipole. This difference gives rise to a weaker distance dependence (z_o^5 vs z_o^8).

C. Comparison of theory and experiment

In Fig. 4, we have plotted γ_{Ao} and γ_{Bo} together as a function of z_o for the aforementioned material combinations. We assume a particle radius of 50 nm and a temperature of $T = 300$ K. We recall that z_o is the distance between the particle center and surface of the substrate. Thus, the minimum allowed physical distance z_o just before the particle contacts the surface is given by the particle's radius—that is, $z_o^{\min} = a$. According to Eq. (19), the total damping coefficient is $\gamma_o = \gamma_{Ao} + \gamma_{Bo}$ (we have discarded γ_{Co} and γ_{Do}). We notice that in Figs. 4(a), 4(b), and 4(d) the damping coefficient γ_{Bo} is stronger than γ_{Ao}, and thus $\gamma_o \approx \gamma_{Bo}$. These cases are silver substrate—silver particle, silver substrate—glass particle, and glass particle—glass substrate. On the contrary, for the substrate made of glass and the particle made of silver [Fig. 4(c)], γ_{Ao} is much larger than γ_{Bo}. Therefore, $\gamma_o \approx \gamma_{Ao}$. According to Fig. 4, the damping coefficient for a silver substrate is much weaker than the damping coefficient for a glass substrate. However, recent experiments performed on metal films lead to damping coefficients that are many

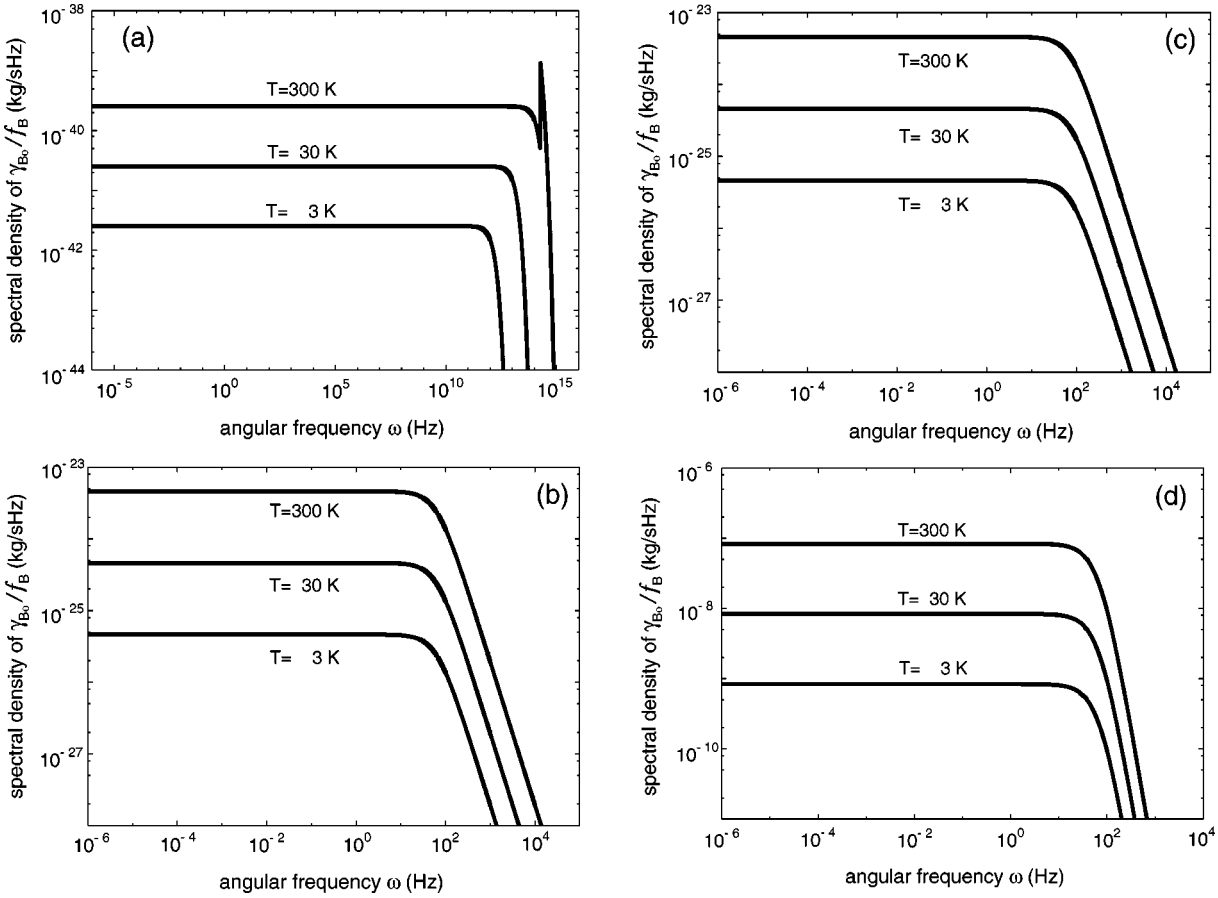

FIG. 3. Normalized spectral density of the damping coefficient γ_{Bo}/f_B as a function of the angular frequency ω [integrand of Eq. (41)] for temperatures $T=3$ K, 30 K, 300 K. $f_B=a^3/z_o^5$ where a and z_o are defined in nanometers. (a) Substrate and particle: Ag; (b) substrate: Ag, particle: SiO_2; (c) substrate: SiO_2, particle: Ag; (d) particle and substrate: SiO_2.

orders of magnitude larger than the values obtained by theoretical predictions. This discrepancy was already pointed out in several previous studies [12,16,24]. However, in the experiments performed in Refs. [20–22] the substrate did *not* consist of a bulk conductor but of a metal film with a thickness of a few hundered nanometers deposited on top of a dielectric substrate. Similar procedures were applied for the fabrication of nanoscale probes that are represented in our study by an oscillating particle; e.g., in Ref. [20] a silicon tip (curvature radius 1 μm) covered with gold was used.

According to our theory, the damping coefficient for a glass substrate is determined by the low-frequency region of less than 100 Hz. However, in this frequency regime the skin depth d_{skin} of a typical metal $[d_{\text{skin}}=c\sqrt{2\varepsilon_o/(\sigma\omega)}]$ is considerably larger than the metal film thickness used in previous experiments. For example, for silver one finds a skin depth of $d_{\text{skin}}^{\text{Ag}}\approx 0.163/\sqrt{\omega\ (\text{Hz})}$ m. Therefore, it is likely that experimental measurements performed on metal films do not reflect the properties of the metal but of the underlying dielectric substrate. If a planar film with thickness d_f and dielectric constant $\epsilon_3(\omega)$ lies on a substrate with dielectric constant $\epsilon_2(\omega)$ as is depicted in the inset of Fig. 1, the system response is similar to the single-interface case if one replaces the reflection coefficients r_{12}^{ζ} $(\zeta=s,p)$ by

$$\rho^{\zeta}=\frac{r_{13}^{\zeta}+r_{32}^{\zeta}\exp(2i\omega d_f\beta_3/c)}{1-r_{31}^{\zeta}r_{32}^{\zeta}\exp(2i\omega d_f\beta_3/c)}. \tag{44}$$

Here, r_{ij}^{ζ} and β_i are defined by Eqs. (B7)–(B9), respectively. For evanescent fields—i.e., in the limit of $q\gg q_m$ (q is the normalized transverse wave number and $q_m\equiv\text{Max}[\sqrt{|\epsilon_i|}]$, $i=1,2,3$)—Eq. (44) can be approximated as (p polarization)

$$\rho^{p}\approx\frac{r_{13}^{p}+r_{32}^{p}\exp(-2\omega d_f q/c)}{1-r_{31}^{p}r_{32}^{p}\exp(-2\omega d_f q/c)}. \tag{45}$$

TABLE II. Normalized damping coefficient γ_{Bo}/f_B for a spherical particle calculated from Eq. (41) for several temperatures ($T=3$ K, 30 K, 300 K). $f_B=a^3/z_o^5$ where a and z_o are defined in nanometers.

Substrate	Particle	γ_{Bo}/f_B (kg/s)		
		3 K	30 K	300 K
Silver	Silver	3.28×10^{-30}	3.28×10^{-28}	1.01×10^{-25}
Silver	Glass	4.69×10^{-24}	4.71×10^{-23}	6.01×10^{-22}
Glass	Silver	5.66×10^{-24}	5.69×10^{-23}	7.64×10^{-22}
Glass	Glass	4.65×10^{-08}	4.65×10^{-07}	4.65×10^{-06}

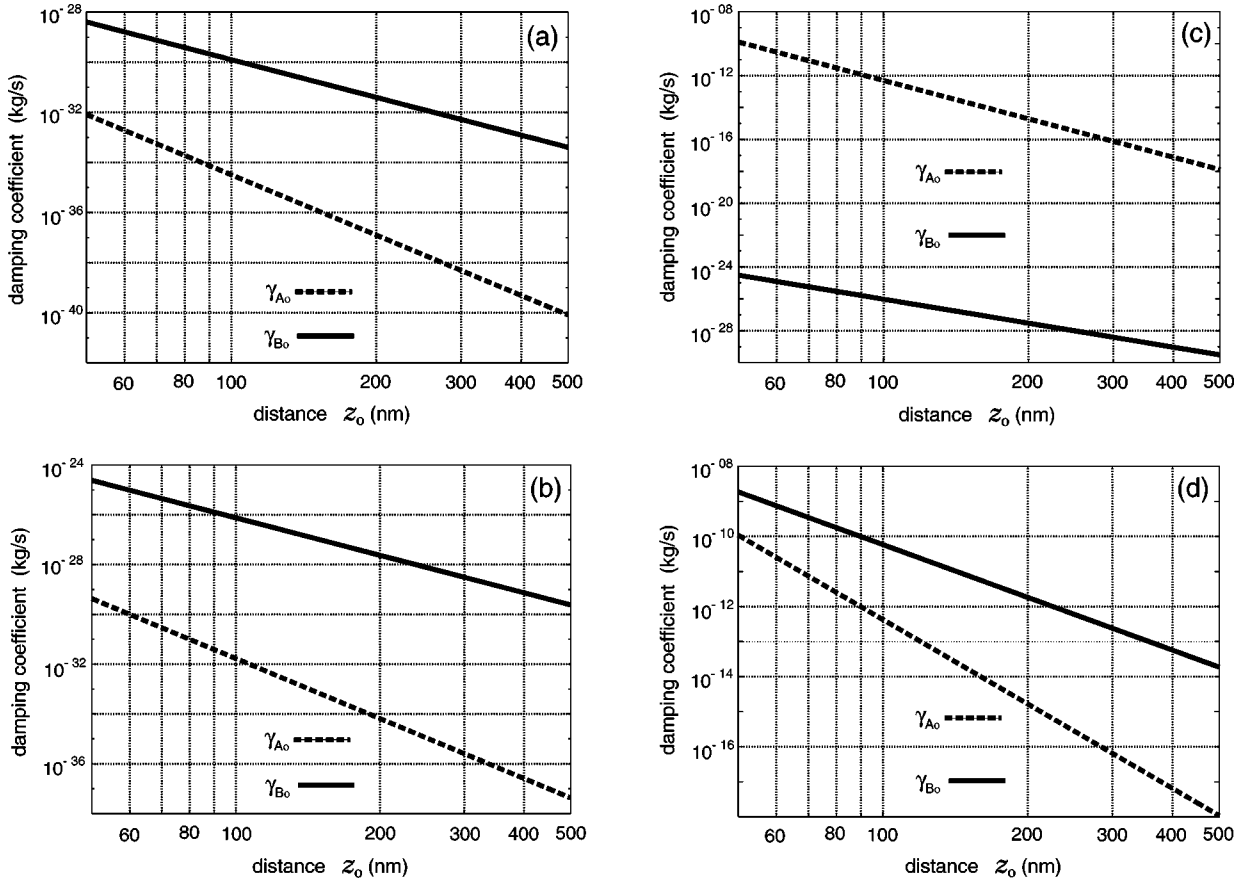

FIG. 4. Damping coefficients γ_{Ao} and γ_{Bo} as a function of z_o from Eqs. (36) and (41), respectively. The radius of the particle is $a=50$ nm and the temperature is $T=300$ K. (a) Substrate and particle: Ag; (b) substrate: Ag, particle: SiO_2; (c) substrate: SiO_2, particle: Ag; (d) particle and substrate: SiO_2.

We can distinguish two regimes (1) $q \ll q_o$ and (2) $q \gg q_o$, with $q_o \equiv c/(2\omega d_f)$. In the former case, Eq. (45) reduces to $\rho^p \approx r_{12}^p$; that is, the response is given by the underlying interface. On the other hand, for $q \gg q_o$, Eq. (45) can be approximated as $\rho^p \approx r_{13}^p$; namely, the response is determined by the topmost interface. In the low-frequency regime and for a metallic layer with a thickness of a few hundreds of nanometers we have $q_o/q_m \gg 1$, where $q_m = \sqrt{\sigma/(\varepsilon_o \omega)}$. In this case we are in regime (1) and we obtain

$$\frac{q_o}{q_m} = \frac{c\sqrt{\varepsilon_o}}{2d_f\sqrt{\sigma\omega}} = \frac{\sqrt{2}d_{\text{skin}}}{4d_f}. \tag{46}$$

For a single glass interface it was shown that the frequency range contributing to the damping coefficient is about $<\sim 100$ Hz. In this low-frequency regime the skin depth of silver is $d_{\text{skin}}^{\text{Ag}} >\sim 1.63$ cm and for a silver layer with thickness $d_f = 250$ nm we find a value $q_o/q_m >\sim 2.5\times 10^4$. Consequently, we confirm our previous statement that measurements performed on finite metal films deposited on dielectric substrates are insensitive to the metal film and are dominated by the properties of the underlying dielectric.

To compare our theory with experiment we consider the results obtained in Ref. [20] where a 250-nm-thick gold film was deposited on a mica substrate. Friction measurements were performed with a 200-nm gold-coated silicon tip with radius ≈ 1 μm. For $T=300$ K and a probe-sample distance of 10 nm a friction coefficient of $\gamma = 1.5\times 10^{-13}$ kg/s is reported. According to our hypothesis that friction is insensitive to the metal coatings we have to translate the probe-sample distances as

$$z_o = s + (\text{surface layers}) + (\text{tip radius}) = s + 1450 \text{ nm}. \tag{47}$$

Here, s is the tip's apex-surface separation, and we assumed that the silicon tip can be approximated by a sphere of radius $a=1$ μm. For the relevant low-frequency regime, this particle size falls well into the electrostatic limit. However, the approximation of a tip geometry by a spherical particle will introduce some errors in our estimates. For a rough comparison, we consider a particle and substrate made of glass. While mica has a higher resistivity than glass, the situation is opposite for undoped silicon. We assume that these deviations roughly compensate and thus we take the values from Tables I and II. For a distance of $z_o = 1460$ nm ($s=10$ nm) we obtain $\gamma_{Ao} = 1.3\times 10^{-14}$ kg/s and $\gamma_{Bo} = 7\times 10^{-13}$ kg/s, respectively. These values are in rough agreement with the experimental value reported in Ref. [20].

In fact, this order-of-magnitude agreement should encourage more dedicated experiments to prove (or disprove) the

here developed theory. It is also remarkable that the coordinate offset between s and z_o according to Eq. (47) weakens the here calculated strong distance dependence of z_o^{-5} and z_o^{-8}. This coordinate translation results in a series of weaker power dependences, leading to qualitative agreement with the measured dependence of $s^{-1.3}$ in Ref. [20]. A closer look at the experimental curves shows that the distance dependence cannot be fitted by a uniform power dependence over the entire measurement range. This could well originate from the coordinate translation of Eq. (47). Deviations between theory and experiment can partially be attributed to the failure of the spherical tip model. In any case, more dedicated experiments are necessary to investigate whether the here developed theory provides the correct explanation for the observed increase of damping near material boundaries. Experimental damping coefficients have to be compared for dielectric and solid metal substrates with well-defined crystal structure. To avoid problems with surface contamination *in situ* sputtering of the tip and surface in ultrahigh-vacuum conditions is necessary. Measurements on top of a superconducting material should lead to no change in damping coefficient if the superconductor is cooled below the critical temperature. The linear-velocity damping coefficient vanishes at $T=0$ K. Residual damping at this temperature may arise from higher-order terms that are *not* linear in the particle's velocity.

V. CONCLUSIONS

We calculated the linear-velocity damping coefficient γ_o for a classical oscillator interacting through fluctuating electromagnetic fields with the environment. In the lowest-order approximation, γ_o is given by the sum of four terms of which only two are significant, $\gamma_{\mathrm{A}o}$ and $\gamma_{\mathrm{B}o}$. $\gamma_{\mathrm{A}o}$ is related to the correlation of the *induced* electric dipole with the exterior fluctuating thermal field, and $\gamma_{\mathrm{B}o}$ is related to the correlation of the *fluctuating* electric dipole with the exterior fluctuating thermal field. In the nonretarded limit, $\gamma_{\mathrm{A}o}$ is mainly sensitive to the dielectric properties of the substrate. On the other hand, the damping coefficient $\gamma_{\mathrm{B}o}$ is sensitive to both the properties of particle and surface. In the nonretarded limit, $\gamma_{\mathrm{B}o}$ reproduces the result derived in Ref. [14].

We find that the damping coefficient for an oscillator above a dielectric substrate is many orders of magnitude larger than for an oscillator above a metal surfaces. This arises from the very different conductive properties of a dielectric and a metal. Our theory shows that the damping coefficient for a dielectric surface is defined by frequencies smaller than 100 Hz. The order of theoretical values is in rough agreement with the measurements in Ref. [20]. The here developed theory provides guidance for future experiments and shows that there are trade-offs to miniaturization because of increased dissipation at short distances. Also, the theory should be of importance for the design of nanoscale mechanical systems and for the choice of favorable materials.

Note added. Recently, a study was published discussing the influence of a surface adsorbate layer on thermal friction [41]. Another article that appeared after our submission discusses free-space damping [42]. It can be shown that this limit can be derived from our damping coefficient $\gamma_{\mathrm{B}o}$ (cf. Appendix G).

ACKNOWLEDGMENTS

The authors thank Khaled Karrai for inspiring this work and for his valuable input. This work was funded by the U.S. Department of Energy through Grant No. DE-FG02-01ER15204 and by Fulbright-CONACyT (J.R.Z-S).

APPENDIX A: FOURTH-ORDER CORRELATION FUNCTION FOR A GAUSSIAN PROCESS

Let $z_1(\mathbf{r}_1,t)$, $z_2(\mathbf{r}_2,t)$, $z_3(\mathbf{r}_3,t)$, and $z_4(\mathbf{r}_4,t)$ be analytical signals of a stationary Gaussian stochastic process. The real and imaginary parts of each signal are related by the Hilbert transform [28]. We define Q as

$$Q\equiv\langle\tilde{z}_1^*(\mathbf{r}_1,\omega_1)\tilde{z}_2^*(\mathbf{r}_2,\omega_2)\tilde{z}_3(\mathbf{r}_3,\omega_3)\tilde{z}_4(\mathbf{r}_4,\omega_4)\rangle, \quad \text{(A1)}$$

where

$$\tilde{z}_i(\mathbf{r},\omega)=\frac{1}{2\pi}\int_{-\infty}^{\infty} z_i(\mathbf{r},t)\mathrm{e}^{\mathrm{i}\omega\,\mathrm{t}}dt, \quad i=1,\ldots,4. \quad \text{(A2)}$$

Inserting $\tilde{z}_i$ into Q and making use of the central-limit theorem gives

$$\begin{aligned}Q=&\mathcal{W}_{13}(\mathbf{r}_1,\mathbf{r}_3,\omega_3)\mathcal{W}_{24}(\mathbf{r}_2,\mathbf{r}_4,\omega_4)\,\delta(\omega_3-\omega_1)\,\delta(\omega_4-\omega_2)\\&+\mathcal{W}_{14}(\mathbf{r}_1,\mathbf{r}_4,\omega_4)\mathcal{W}_{23}(\mathbf{r}_2,\mathbf{r}_3,\omega_3)\,\delta(\omega_4-\omega_1)\\&\times\delta(\omega_3-\omega_2),\end{aligned} \quad \text{(A3)}$$

with

$$\mathcal{W}_{ij}(\mathbf{r},\mathbf{r}',\omega)\equiv\frac{1}{2\pi}\int_{-\infty}^{\infty}\Gamma_{ij}(\mathbf{r},\mathbf{r}';\tau)\mathrm{e}^{\mathrm{i}\omega\,\tau}d\tau \quad \text{(A4)}$$

and

$$\Gamma_{ij}(\mathbf{r},\mathbf{r}';t'-t=\tau)=\langle z_i^*(\mathbf{r},t)z_j(\mathbf{r}',t')\rangle. \quad \text{(A5)}$$

APPENDIX B: EXPRESSIONS IN γ_{A}

The explicit expressions for $f_{\mathrm{A}1}(z_o,\omega)$, $f_{\mathrm{A}2}(z_o,\omega)$, $f_{\mathrm{A}3}(z_o,\omega)$, $g_{\mathrm{A}1}(z_o,\omega)$, and $g_{\mathrm{A}2}(z_o,\omega)$ are

$$\begin{aligned}f_{\mathrm{A}1}(z_o,\omega)=\frac{\hbar\omega^3}{8\pi^2c^3\varepsilon_o}\Big(&\mathrm{Im}[\mathrm{i}I_{1-1}^s(z_o,\omega)]\\&-\mathrm{Im}[\mathrm{i}I_{11}^p(z_o,\omega)]+\frac{4}{3}\Big),\end{aligned} \quad \text{(B1)}$$

$$f_{\mathrm{A}2}(z_o,\omega)=\frac{\hbar\omega^3}{4\pi^2c^3\varepsilon_o}\Big(\mathrm{Im}[\mathrm{i}I_{3-1}^p(z_o,\omega)]+\frac{2}{3}\Big), \quad \text{(B2)}$$

$$f_{\mathrm{A3}}(z_o,\omega)=\frac{\hbar\omega^4}{8\pi^2c^4\varepsilon_o}\mathrm{Im}[I^p_{30}(z_o,\omega)], \tag{B3}$$

$$g_{\mathrm{A1}}(z_o,\omega)=\frac{\hbar\omega^5}{8\pi^2c^5\varepsilon_o}\Big(\mathrm{Im}[\mathrm{i}I^s_{3-1}(z_o,\omega)] - \mathrm{Im}[\mathrm{i}I^p_{31}(z_o,\omega)]+\frac{4}{5}\Big), \tag{B4}$$

$$g_{\mathrm{A2}}(z_o,\omega)=\frac{\hbar\omega^5}{8\pi^2c^5\varepsilon_o}\Big(\mathrm{Im}[\mathrm{i}I^p_{5-1}(z_o,\omega)]+\frac{8}{15}\Big). \tag{B5}$$

Here, $I^{\zeta}_{nm}(z_o,\omega)$ is defined as

$$I^{\zeta}_{nm}(z_o,\omega)\equiv\int_0^\infty r^{\zeta}_{12}q^n\beta_1^m e^{\mathrm{i}2\omega z_o\beta_1/c}dq, \tag{B6}$$

where q is a dimensionless parameter and r^{ζ}_{ij} are the Fresnel reflection coefficients for polarizations $\zeta=s,p$ defined as

$$r^s_{ij}=\frac{\beta_i-\beta_j}{\beta_i+\beta_j}, \tag{B7}$$

$$r^p_{ij}=\frac{\beta_i\epsilon_j-\beta_j\epsilon_i}{\beta_i\epsilon_j+\beta_j\epsilon_i}, \tag{B8}$$

$$\beta_i=\sqrt{\epsilon_i(\omega)-q^2}. \tag{B9}$$

The index i refers to the medium of incidence and the index j designates the medium of transmittance.

APPENDIX C: EXPRESSIONS IN γ_{B}

The explicit expression for $g_{\mathrm{B}}(z_o,\omega)$ is

$$g_{\mathrm{B}}(z_o,\omega)=\frac{\hbar\omega^5}{8\pi^2c^5\varepsilon_o}\Big(\mathrm{Im}[\mathrm{i}I^s_{3-1}(z_o,\omega)]+\mathrm{Im}[-\mathrm{i}I^p_{31}(z_o,\omega)] + \mathrm{Im}[\mathrm{i}I^p_{5-1}(z_o,\omega)]+\frac{4}{3}\Big). \tag{C1}$$

APPENDIX D: EXPRESSIONS IN γ_{C}

The explicit expressions for $f_{\mathrm{C}}(z_o,\omega)$ and $g_{\mathrm{C}}(z_o,\omega)$ are

$$f_{\mathrm{C}}(z_o,\omega)=\frac{\hbar\omega^3}{8\pi^2c^3\varepsilon_o}\Big(\mathrm{Im}[\mathrm{i}I^s_{1-1}(z_o,\omega)]+\mathrm{Im}[-\mathrm{i}I^p_{11}(z_o,\omega)] + 2\,\mathrm{Im}[\mathrm{i}I^p_{3-1}(z_o,\omega)]+\frac{8}{3}\Big), \tag{D1}$$

$$g_{\mathrm{C}}(z_o,\omega)=\frac{\hbar\omega^8}{64\pi^3c^8\varepsilon_o^2}|I^p_{30}(z_o,\omega)|^2. \tag{D2}$$

APPENDIX E: EXPRESSIONS IN γ_{D}

The explicit expression for $g_{\mathrm{D}}(z_o,\omega)$ is

$$f_{\mathrm{D}}(z_o,\omega)=\frac{\hbar^2\omega^8}{8\pi^4c^8\varepsilon_o^2}\mathrm{Im}^2[I^p_{30}(z_o,\omega)]. \tag{E1}$$

APPENDIX F: DISCUSSION OF γ_{CO} AND γ_{DO}

In the nonretarded limit, $\gamma_{\mathrm{C}o}$ and $\gamma_{\mathrm{D}o}$ are

$$\gamma_{\mathrm{C}o}=\frac{27\hbar^2}{1024\pi k_{\mathrm{B}}T}\frac{a^9}{z_o^{11}}\int_0^\infty|\xi(\omega)|^2\mathrm{Im}[\xi(\omega)] \times\left|\frac{\epsilon_2(\omega)-1}{\epsilon_2(\omega)+1}\right|^2\mathrm{Im}\left[\frac{\epsilon_2(\omega)-1}{\epsilon_2(\omega)+1}\right]\eta(\omega,T)d\omega, \tag{F1}$$

$$\gamma_{\mathrm{D}o}=\frac{9\hbar^2}{32\pi k_{\mathrm{B}}T}\frac{a^6}{z_o^8}\int_0^\infty\mathrm{Im}^2[\xi(\omega)]\mathrm{Im}^2\left[\frac{\epsilon_2(\omega)-1}{\epsilon_2(\omega)+1}\right]\eta(\omega,T)d\omega. \tag{F2}$$

In the low-frequency limit, the frequency-dependent terms in $\gamma_{\mathrm{C}o}$ resemble those of $\gamma_{\mathrm{B}o}$. However, the different particle volume, distance dependence (z_o^{-11}), and magnitude of the proportionality constant make this contribution neglible in comparison with the other terms. On the other hand, the damping coefficient $\gamma_{\mathrm{D}o}$ is proportional to ω^2 in the low-frequency limit which makes $\gamma_{\mathrm{D}o}$ small compared with other terms.

APPENDIX G: FREE-SPACE DAMPING

Thermal friction is present even in free space. The free-space damping coefficient is obtained from Eqs. (22) and (26) in the limit $\omega z_o/c\to\infty$. The free-space damping coefficient γ_o^{F} turns out to be

$$\gamma_o^{\mathrm{F}}=\gamma_{\mathrm{A}o}^{\mathrm{F}}+\gamma_{\mathrm{B}o}^{\mathrm{F}}, \tag{G1}$$

$$\gamma_{\mathrm{A}o}^{\mathrm{F}}=\frac{\hbar^2}{18\pi^3c^8\varepsilon_o^2k_{\mathrm{B}}T}\int_0^\infty|\alpha(\omega)|^2\omega^8\eta(\omega,T)d\omega, \tag{G2}$$

$$\gamma_{\mathrm{B}o}^{\mathrm{F}}=\frac{\hbar^2}{3\pi^2c^5\varepsilon_ok_{\mathrm{B}}T}\int_0^\infty\mathrm{Im}[\alpha(\omega)]\omega^5\eta(\omega,T)d\omega. \tag{G3}$$

This expression is general since it does not assume any particular particle's polarizability $\alpha(\omega)$. Equation (G2) reproduces the damping coefficient derived in Ref. [35] if the radiative reaction force is included in the expression for the classical polarizability. On the other hand, Eq. (G3) appears to be unreported so far.

[1] H.B. Chan, V.A. Aksyuk, R.N. Kleiman, D.J. Bishop, and F. Capasso, Science **291**, 1941 (2001).
[2] H.B. Chan, V.A. Aksyuk, R.N. Kleiman, D.J. Bishop, and F. Capasso, Phys. Rev. Lett. **87**, 211801 (2001).
[3] D.J. Wineland, C. Monroe, W.M. Itano, D. Leibfried, B.E. King, and D.M. Meekhof, J. Res. Natl. Inst. Stand. Technol. **103**, 259 (1998).
[4] A. Einstein and L. Hopt, Ann. Phys. (Leipzig) **33**, 1105 (1910).
[5] A. Einstein and O. Stern, Ann. Phys. (Leipzig) **40**, 551 (1913).
[6] P. W. Milonni, *The Quantum Vacuum. An Introduction to Quantum Electrodynamics* (Academic Press, San Diego, 1994).
[7] P.W. Milonni and M.L. Shih, Am. J. Phys. **59**, 684 (1991).
[8] E.V. Teodorovich, Proc. R. Soc. London, Ser. A **362**, 71 (1978).
[9] L.S. Levitov, Europhys. Lett. **8**, 499 (1989).
[10] G. Barton, Ann. Phys. (N.Y.) **245**, 361 (1996).
[11] J.B. Pendry, J. Phys.: Condens. Matter **9**, 10 301 (1997).
[12] A.I. Volokitin and B.N.J. Persson, J. Phys. C **11**, 345 (1999).
[13] W.L. Schaich and J. Harris, J. Phys. F: Met. Phys. **11**, 65 (1981).
[14] M.S. Tomassone and A. Widom, Phys. Rev. B **56**, 4938 (1997).
[15] A.A. Kyasov and G.V. Dedkov, Surf. Sci. **491**, 124 (2001).
[16] A.I. Volokitin and B.N.J. Persson, Phys. Rev. B **65**, 115419 (2002).
[17] G.V. Dedkov and A.A. Kyasov, Phys. Solid State **44**, 1809 (2002).
[18] G.V. Dedkov and A.A. Kyasov, Phys. Low-Dim. Struc. **1**, 1 (2003).
[19] K. Karrai and I. Tiemann, Phys. Rev. B **62**, 13 174 (2000).
[20] B.C. Stipe, H.J. Mamin, T D. Stowe, T.W. Kenny, and D. Rugar, Phys. Rev. Lett. **87**, 096801 (2001).
[21] I. Dorofeyev, H. Fuchs, G. Wenning, and B. Gotsmann, Phys. Rev. Lett. **83**, 2402 (1999).
[22] B. Gotsmann and H. Fuchs, Phys. Rev. Lett. **86**, 2597 (2001).
[23] F.J. Giessibl, M. Herz, and J. Mannhart, PNAS **99**, 12 006 (2002).
[24] B.N.J. Persson and A.I. Volokitin, Phys. Rev. Lett. **84**, 3504 (2000).
[25] H.B. Callen and T.A. Welton, Phys. Rev. **83**, 34 (1951).
[26] R. Kubo, M. Toda, and N. Hashizume, *Statistical Mechanics II: Nonequilibrium Statistical Mechanics* (Springer-Verlag, Berlin, 1985), Chap. 1, pp. 1–39.
[27] S. M. Rytov, Y. A. Kravtsov, and V. I. Tatarskii, *Principles of Statistical Radiophysics* (Springer-Verlag, Berlin, 1987), Vol. III, Chap. 3, pp. 109–173.
[28] L. Mandel and E. Wolf, *Optical Coherence and Quantum Optics* (Cambridge University Press, New York, 1995), Chap. 2.
[29] L. Novotny, in *Near-field Optics and Surface Plasmon Polaritons*, edited by S. Kawata (Springer-Verlag, Berlin, 2001), pp. 123–141.
[30] C. Henkel, K. Joulain, J.-P. Mulet, and J.-J. Greffet, J. Opt. A **4**, S109 (2002).
[31] W. Eckhardt, Opt. Commun. **41**, 305 (1982).
[32] H.T. Dung, L. Knöll, and D. Welsch, Phys. Rev. A **57**, 3931 (1998).
[33] G.S. Agarwal, Phys. Rev. A **11**, 230 (1975).
[34] C. T. Tai, *Dyadic Green's Functions in Electromagnetic Theory* (Intext Educational Publishers, Scranton, 1971).
[35] T.H. Boyer, Phys. Rev. **182**, 1374 (1969).
[36] D. W. Lynch and W. R. Hunter, in *Handbook of Optical Constants of Solids*, edited by E.D. Palik (Academic Press, San Diego, 1985), pp. 350–357.
[37] M.A. Ordal, L.L. Long, R.J. Bell, S.E. Bell, R.R. Bell, R.W. Alexander, Jr., and C.A. Ward, Appl. Opt. **22**, 1099 (1983).
[38] M.N. Afsar and K.J. Button, IEEE Trans. Microwave Theory Tech. **31**, 217 (1983).
[39] H. R. Philipp, in *Handbook of Optical Constants of Solids*, edited by E. D. Palik (Academic Press, San Diego, 1985), pp. 749–763.
[40] *Materials Science and Engineering Handbook*, 3rd ed., edited by J.F. Shackelford and W. Alexander (CRC Press, Boca Raton, 2001).
[41] A.I. Volokitin and B.N.J. Persson, Phys. Rev. Lett. **91**, 106101 (2003).
[42] V. Mkrtchian, V.A. Parsegian, R. Podgornik, and W.M. Saslow, Phys. Rev. Lett. **91**, 220801 (2003).